

Supporting Information

B–N bond-doped multiple resonance emitter with extended π -conjugation for narrowband sky-blue OLED exhibiting low efficiency roll-off

Jianping Zhou,^{1,#} Hai Zhang,^{1,#} Qi Wang,¹ Danrui Wan,² Guoyun Meng,^{2,*} Dongdong Zhang,¹ Lian Duan^{1,*}

¹Key Laboratory of Organic Optoelectronics and Molecular Engineering of Ministry of Education, Department of Chemistry, Tsinghua University, Beijing 100084, China

²School of Chemical Science and Technology, Yunnan University, Kunming 650091, China

† Correspondence to: mengguoyun@ynu.edu.cn; duanl@mail.tsinghua.edu.cn

Table of Contents

1. Experimental section	1
1.1 General information	1
1.2 Computational methods	1
1.3 Measurement of absorption and emission characteristics	1
1.4 Electrochemical measurements	2
1.5 The rate constants calculation	2
1.6 Device fabrication and measurement of EL characteristics	2
2. Synthesis and characterization	3
3. Supplementary figures and tables	4
4. References	9

1. Experimental Section

1.1 General Information. Reagents for the reactions, purification, and measurements were procured from Shanghai Bide Medical Technology Co. Ltd. Materials for device fabrication were obtained from Jilin Optical and Electronic Materials Co. Ltd., all used without further purification. Other reagents and solvents were obtained from commercial sources without further purification. $^1\text{H-NMR}$ and $^{13}\text{C-NMR}$ spectra were recorded on a Bruker Avance 400 MHz spectrometer at room temperature in deuterated chloroform, with tetramethylsilane as the internal standard. MALDI-TOF-MS data was acquired on a Shimadzu AXIMA Performance MALDI-TOF instrument in positive detection mode. Thermogravimetry (TG) was conducted on a Netzsch STA 449 F3 thermal analyzer at a heating rate of $10\text{ }^\circ\text{C min}^{-1}$ under N_2 flow. UV-vis absorption and PL spectra were measured using UV-2600 (Shimadzu) and FluoroMax-4P (Horiba) instruments, respectively. The photoluminescence quantum yields (PLQYs) were obtained with an absolute photoluminescence quantum yield measurement system, Hamamatsu C9920-03G, in an integrating sphere.

1.2 Computational methods. The calculations were performed with the Gaussian 09 package, using the density functional theory (DFT) and time-dependent density functional theory (TD-DFT) method with the B3LYP hybrid functional.^[1-3] The structures were optimized using TD-DFT (S_1 state) methods with a 6-31G(d,p) basis set. Natural transition orbital analyses^[4] were also performed to examine the nature of the excited states. Electron-hole analysis was carried out using the Multiwfn software.^[5] The RMSDs of the optimized structures at S_0 and S_1 states were analyzed by VMD software.^[6]

1.3 Measurement of absorption and emission characteristics. $1 \times 10^{-5}\text{ M}$ solutions were prepared by stepwise dilution for solution measurements. Thin films for photophysical characterization were prepared by thermal evaporation on quartz substrates at $1\text{-}2\text{ \AA s}^{-1}$ in a vacuum chamber with a base pressure of $< 10^{-5}$ torr. UV-vis absorption and PL spectra were measured using UV-2600 (Shimadzu) and FluoroMax-4P (Horiba) instruments at 77 and 298 K. The PLQYs were obtained with an absolute photoluminescence quantum yield measurement system Hamamatsu C9920-03G in an integrating sphere. The solution sample was bubbled with nitrogen for 10 minutes before measurement while the films were measured in air. The transient spectra were collected on an Edinburgh Fluorescence Spectroscopy FLS1000.

1.4 Electrochemical measurements. Cyclic voltammetry was performed on a CHI

660 instrument, using a platinum (Pt) electrode as the working electrode, a Pt wire as the auxiliary electrode, and an Ag/Ag⁺ electrode as the reference electrode. The oxidation/reduction potentials were measured in dry dichloromethane solution with 0.1 M of TBAPF₆ (tetrabutylammonium hexafluorophosphate) as a supporting electrolyte at a scan rate of 100 mV s⁻¹.

$$E_{\text{HOMO}} = - (E_{[\text{onset,ox vs. Fc}^+/\text{Fc}]} + 4.8) \text{ (eV)}$$

$$E_{\text{LUMO}} = - (E_{[\text{onset,red vs. Fc}^+/\text{Fc}]} + 4.8) \text{ (eV)}$$

1.5 The rate constants calculation. The prompt fluorescence and delayed fluorescence quantum yield ratio (Φ_{PF} and Φ_{DF}) were determined from the total PL quantum efficiency (Φ_{PL}) and the proportion of the integrated area of each component in the transient spectra to the total integrated area, r_{PF} and r_{DF} are individual component ratio for prompt and delayed fluorescence. The quantum efficiencies and rate constants were determined using the following equations according to Adachi's method.^[7]

$$(1) \Phi_{\text{PF}} = \Phi_{\text{PL}} r_{\text{PF}} \quad r_{\text{PF}} = \tau_1 A_1 / (\tau_1 A_1 + \tau_2 A_2)$$

$$(2) \Phi_{\text{DF}} = \Phi_{\text{PL}} r_{\text{DF}} \quad r_{\text{DF}} = \tau_2 A_2 / (\tau_1 A_1 + \tau_2 A_2)$$

$$(3) k_{\text{r}} = \Phi_{\text{PF}} / \tau_{\text{PF}}$$

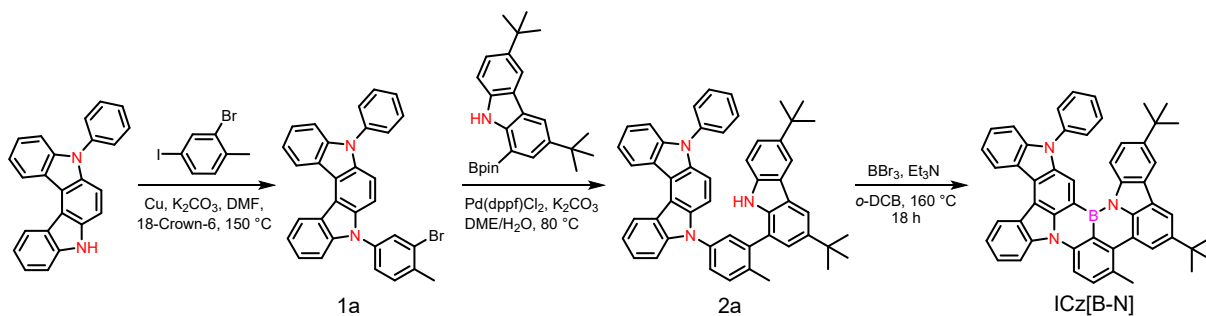
$$(4) k_{\text{ISC}} = 1 - \Phi_{\text{PF}} / \tau_{\text{PF}}$$

$$(5) k_{\text{RISC}} = \Phi_{\text{DF}} / k_{\text{ISC}} \cdot \tau_{\text{PF}} \cdot \tau_{\text{DF}} \cdot \Phi_{\text{PF}}$$

1.6 Device fabrication and measurement of EL characteristics. All compounds were subjected to temperature-gradient sublimation under a high vacuum before use. OLEDs were fabricated on the ITO-coated glass substrates with multiple organic layers sandwiched between the transparent bottom indium-tin-oxide (ITO) anode and the top metal cathode. Before device fabrication, the ITO glass substrates were carefully pre-cleaned. All material layers were deposited by vacuum evaporation in a vacuum chamber with a base pressure of 10⁻⁶ torr. The deposition system permits the fabrication of the complete device structure in a single vacuum pump-down without breaking the vacuum. The deposition rate of organic layers was kept at 0.1~0.2 nm s⁻¹. The doping was conducted by co-evaporation from separate evaporation sources with different evaporation rates. The current density, voltage, luminance, external quantum efficiency, electroluminescent spectra, and other characteristics were measured with a Keithley 2400 source meter and an absolute EQE measurement system in an integrating

sphere at the same time. The EQE measurement system is Hamamatsu C9920-12, which is equipped with Hamamatsu PMA-12 Photonic multichannel analyzer C10027-02 whose longest detection wavelength is 1100 nm.

2. Synthesis and characterization



Scheme. S1. The synthetic route of compound ICz[B-N].

Synthesis of 1a: 2-bromo-4-iodo-1-methylbenzene (1.79 g, 6.02 mmol), 5-phenyl-5,8-dihydroindolo[2,3-c]carbazole (2.0 g, 6.02 mmol), Cu (0.382 g, 6.02 mmol), K₂CO₃ (2.49 g, 18.05 mmol) and 18-Crown-6 (0.477 g, 1.81 mmol) were dissolved in dry DMF (250 mL) at room temperature. The mixture was stirred at 150 °C for 16 h. After cooling to room temperature, the reaction mixture was poured into water. After filtration, the crude product was purified by recrystallization from methanol to afford **1a** as a white solid, 2.68 g, yield of 89%. ¹H NMR (400 MHz, Chloroform-*d*) δ (ppm): 8.96 (d, *J* = 9.9 Hz, 2H), 7.80 (d, *J* = 1.8 Hz, 1H), 7.66 – 7.58 (m, 4H), 7.52 – 7.41 (m, 11H), 2.54 (s, 3H).

Synthesis of 2a: In a 250 mL Schlenk flask, 3,6-di-tert-butyl-1-(4,4,5,5-tetramethyl-1,3,2-dioxaborolan-2-yl)-9H-carbazole (1.11 g, 3.99 mmol) and **1a** (2.0 g, 3.99 mmol) were added. Following the addition of 20 mL dimethoxyethane (DME) and 5 mL aqueous K₂CO₃ (2.76 g, 19.94 mmol) solution, the mixture was degassed for 30 minutes. Subsequently, Pd(dppf)Cl₂ (0.145 g, 0.19 mmol) was added, and the mixture was heated to 80 °C and stirred for 18 hours. The reaction mixture was then poured into water and extracted with CH₂Cl₂ three times. After drying the organic phase over Na₂SO₄ and evaporating the solvent under vacuum, the crude product was purified by flash chromatography on silica gel using petroleum ether / CH₂Cl₂ (5:1, v/v) to give **2a** as a white solid (2.32 g, 80.1% yield). ¹H NMR (400 MHz, Chloroform-*d*) δ (ppm): 8.90 (d, *J* = 8 Hz, 2H), 8.02 (d, *J* = 4 Hz, 2H), 7.68 (s, 1H), 7.63 (s, 1H), 7.58 – 7.52 (m, 8H), 7.44 – 7.38 (m, 8H), 7.34 (s, 1H), 7.24 (d, *J* = 8 Hz, 1H), 2.26 (s, 3H), 1.40 (s, 9H), 1.38

(s, 9H).

Synthesis of ICz[B-N]: A mixture of **2a** (2.0 g, 2.86 mmol), triethylamine (Et₃N) (1.59 mL, 11.43 mmol) in dry 1,2-dichlorobenzene (*o*-DCB) (15 mL) was stirred at room temperature for 10 minutes. Then, BBr₃ (0.55 mL, 5.71 mmol) was added dropwise to the reaction mixture. The reaction mixture was heated to 160 °C for 16 hours. After removing the solvent under vacuum, the crude product was washed with hexane and collected by filtration. The obtained solid was sonicated with methanol and collected by filtration to give the title compound **ICz[B-N]** as a blight yellow solid (1.76 g, 87% yield). ¹H NMR (600 MHz, Chloroform-*d*) δ (ppm): 8.91 (d, *J* = 7.6 Hz, 2H), 8.52 (s, 1H), 8.47 (s, 1H), 8.31 (d, *J* = 8.2 Hz, 1H), 8.18 (d, *J* = 8.3 Hz, 1H), 8.10 (s, 1H), 8.03 – 7.98 (m, 2H), 7.56 – 7.39 (m, 11H), 7.02 (d, *J* = 8.5 Hz, 1H), 2.92 (s, 3H), 1.53 (s, 9H), 1.42 (s, 9H). ¹³C NMR (151 MHz, Chloroform-*d*) (ppm): 145.96, 144.55, 142.55, 141.85, 140.88, 139.44, 139.35, 138.18, 137.82, 137.53, 136.95, 136.05, 128.88, 128.07, 127.79, 127.67, 126.70, 126.64, 125.77, 125.62, 124.32, 123.79, 123.67, 123.22, 123.07, 122.47, 121.30, 120.45, 119.62, 116.74, 116.22, 115.86, 115.49, 114.30, 113.55, 112.90, 110.06, 35.27, 34.77, 32.20, 31.84.

3. Supplementary figures and tables

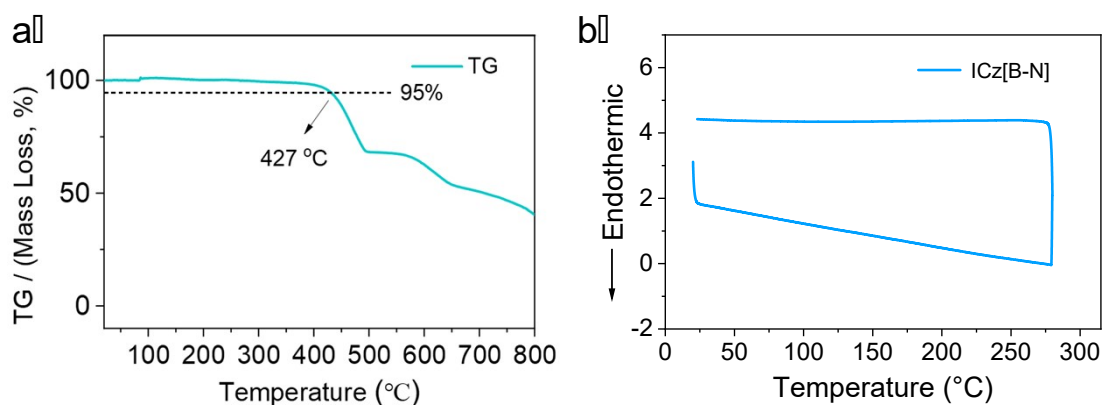


Figure S1. The thermal stability and DSC data of **ICz[B-N]**. The sample was heated and cooled under a nitrogen atmosphere at a rate of 10 °C min⁻¹.

Table S1. Primary orbitals which contribute to the calculated transitions of **ICz[B-N]** (iso = 0.02).

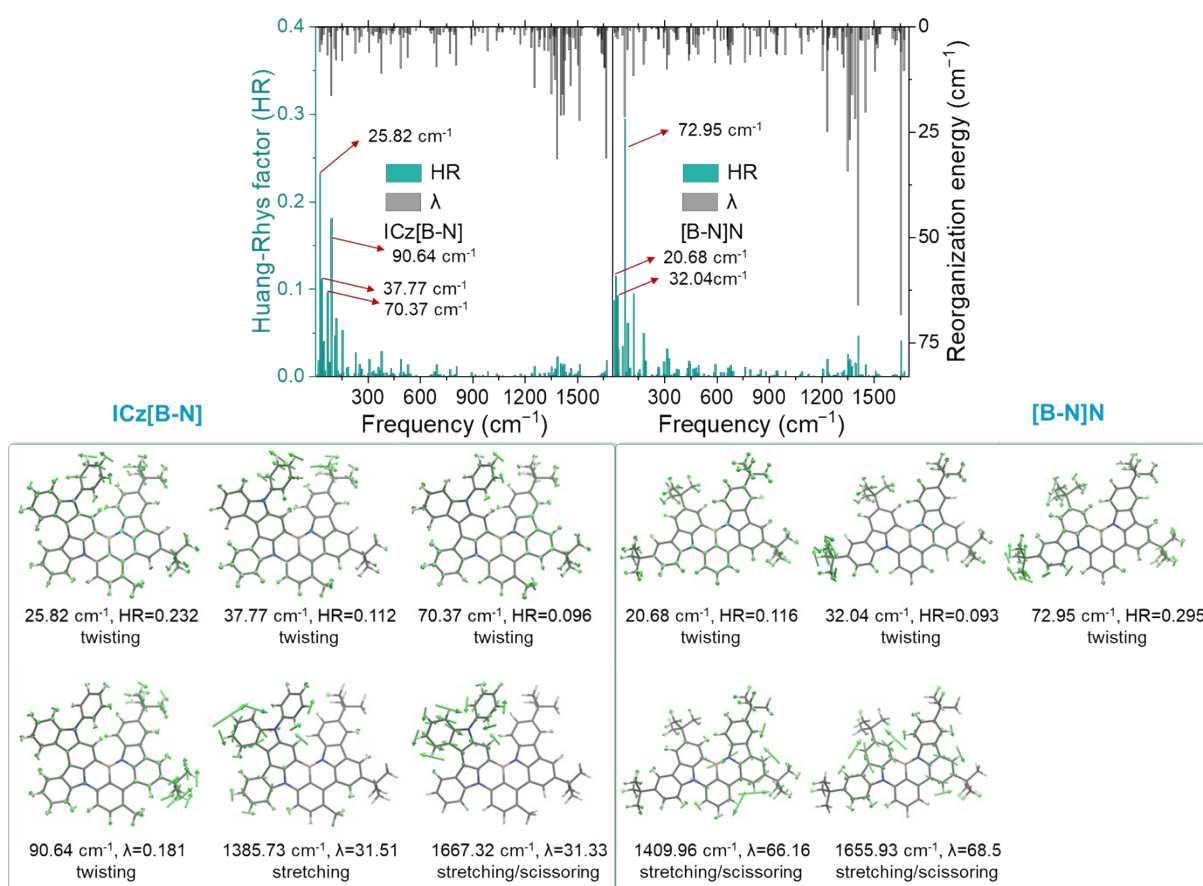
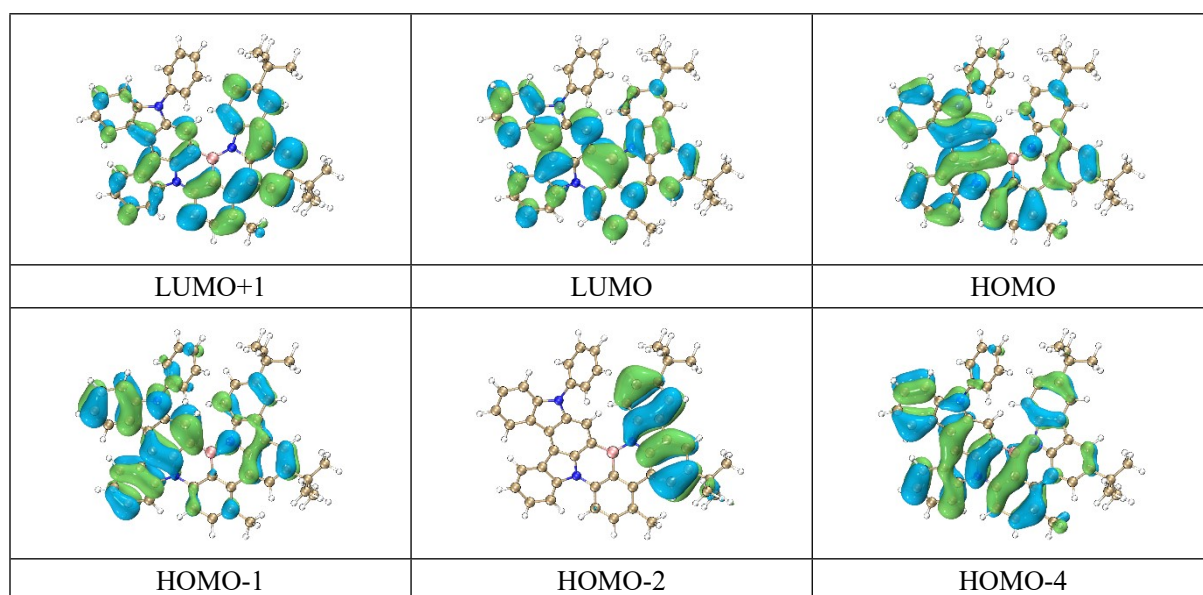


Figure S2. Huang-Rhys (HR) factors and reorganization energy (λ) for ICz[B-N] and parent [B-N]N under different vibrational frequencies.

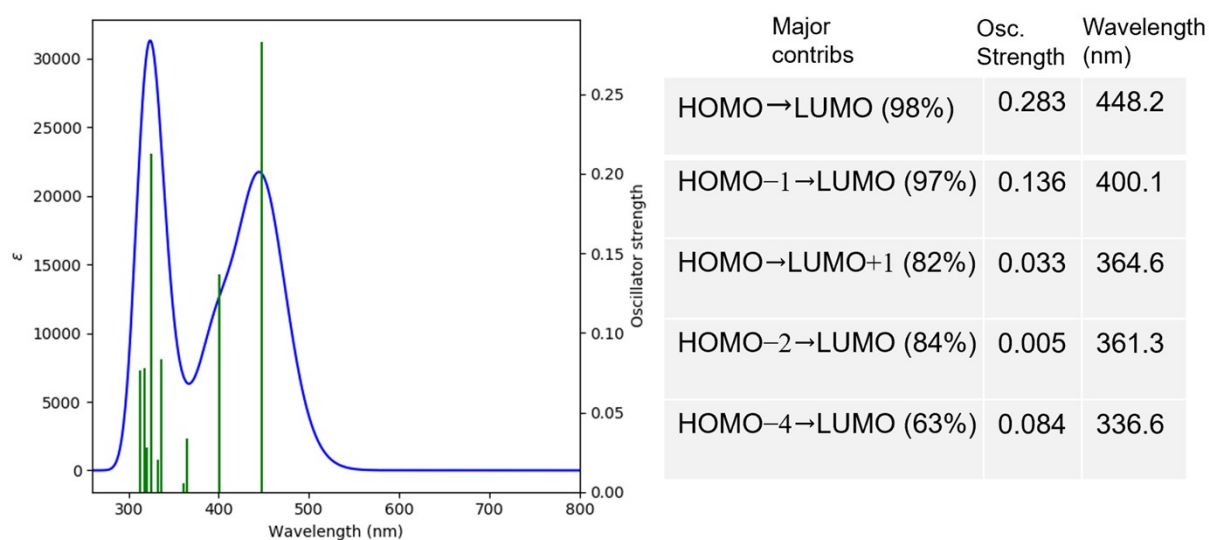


Figure S3. Predicted UV/Vis spectra of **ICz[B-N]** based on TD-DFT calculation.

Table S2. Summary of TD-DFT calculation for **ICz[B-N]** at the S_0 and S_1 structures at the B3LYP/6-31G(d, p) level.

Compound	Optimized Structure	Transition	Wavelength (nm)	Energy (eV)	Oscillator Strength
ICz[B-N]	S_0	$S_0 \rightarrow S_1$	448.18	2.7664	0.2830
		$S_0 \rightarrow T_1$	538.84	2.3010	0
	S_1	$S_1 \rightarrow S_0$	472.41	2.6245	0.2860

Table S3. A comparative of the maximum EQE, FWHM, and wavelength of EL devices for the **ICz[B-N]** and other B-N based MR emitters.

Emitter	λ_{PL} (nm)	FWHM _{PL} (nm)	λ_{EL} (nm)	FWHM _{EL} (nm)	CIE (x,y)	EQE _{max} (%)	Refs.
ICz[B-N]	484	19	488	24	(0.127, 0.417)	15.0	This work
m[B-N]N1	481	29	479	27	(0.115, 0.272)	36.0	[8]
m[B-N]N2	491	34	485	33	(0.112, 0.319)	33.4	
[B-N]N	442	19	448	27	(0.151, 0.079)	16.7	[9]
p[B-N]O	488	19	493	25	(0.163, 0.514)	26.3	
p[B-N]NO	522	28	525	31	(0.306, 0.648)	27.6	
p[B-N]N	547	26	552	31	(0.414, 0.571)	24.6	[10]
Cz-DBCz	484	17	487	19	(0.117, 0.367)	31.9	
Cz-DBTPA	478	17	481	18	(0.116, 0.264)	27.1	
PhO-DBCz	469	18	473	27	(0.126, 0.208)	29.5	[11]
RBNN	617	38	617	48	(0.667, 0.332)	36.6	
[B-N]N1	445	19	-	-	-	-	

[B-N]N2	438	16	441	20	(0.152, 0.046)	20.3	
[B-N]N3	458	37	459	40	(0.141, 0.105)	19.6	
[B-N]N4	463	27	466	30	(0.134, 0.133)	22.1	
DABNA-3B	470	19	475	25	-	33.8	[14]
BCzBN-3B	482	16	493	22	-	42.6	
3B-tCz	427	16	436	41	(0.155, 0.065)	6.9	[15]
3B-DPA	437	13	440	14	(0.154, 0.031)	18.7	

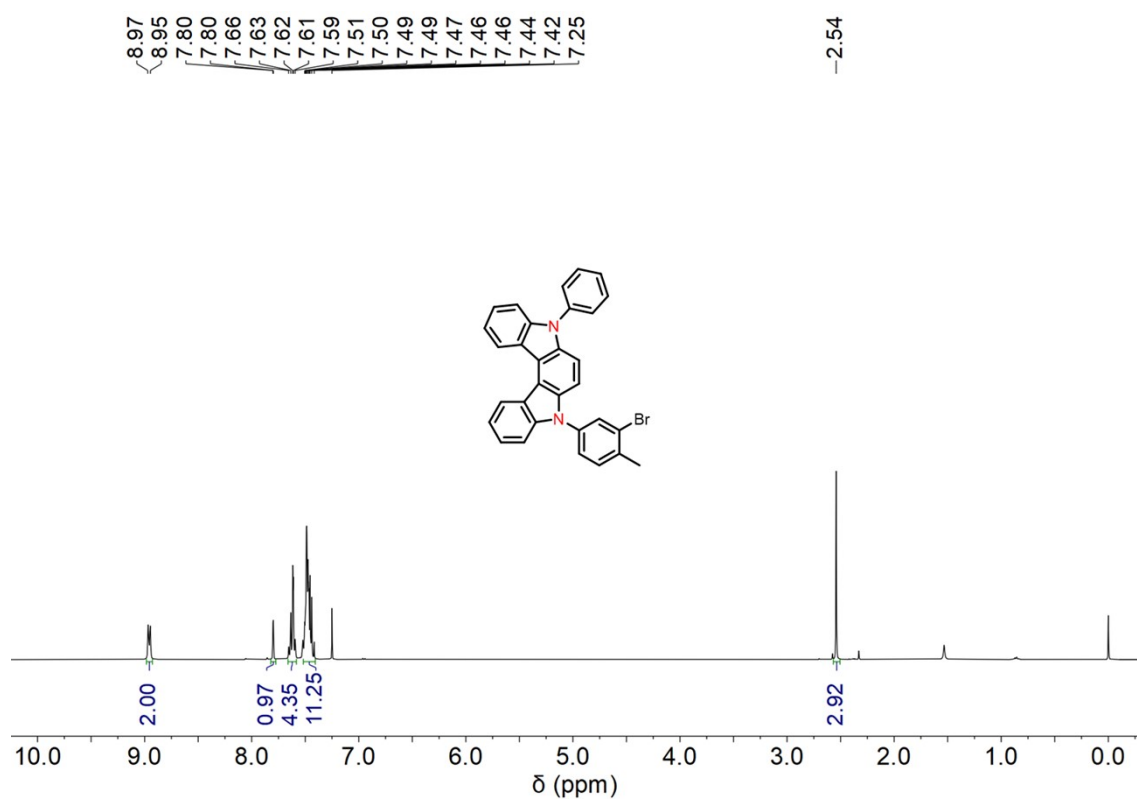


Figure S4. ^1H NMR spectrum of **1a** in CDCl_3 .

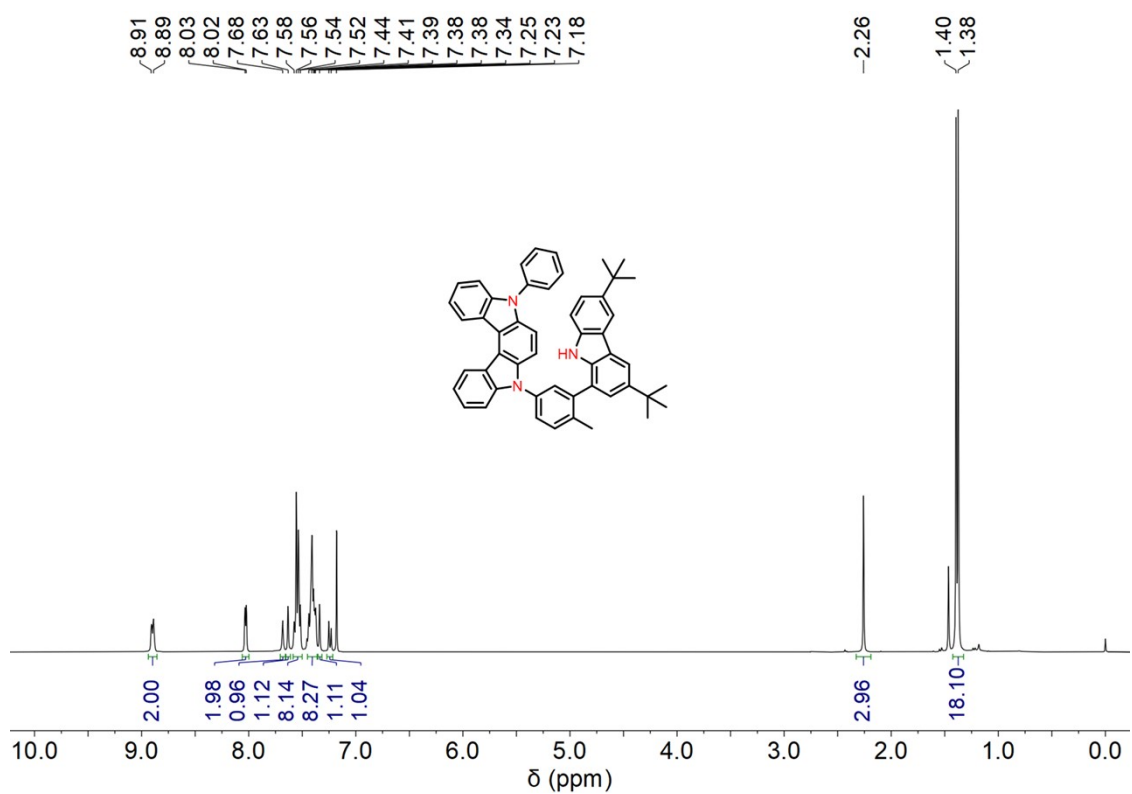


Figure S5. ^1H NMR spectrum of **2a** in CDCl_3 .

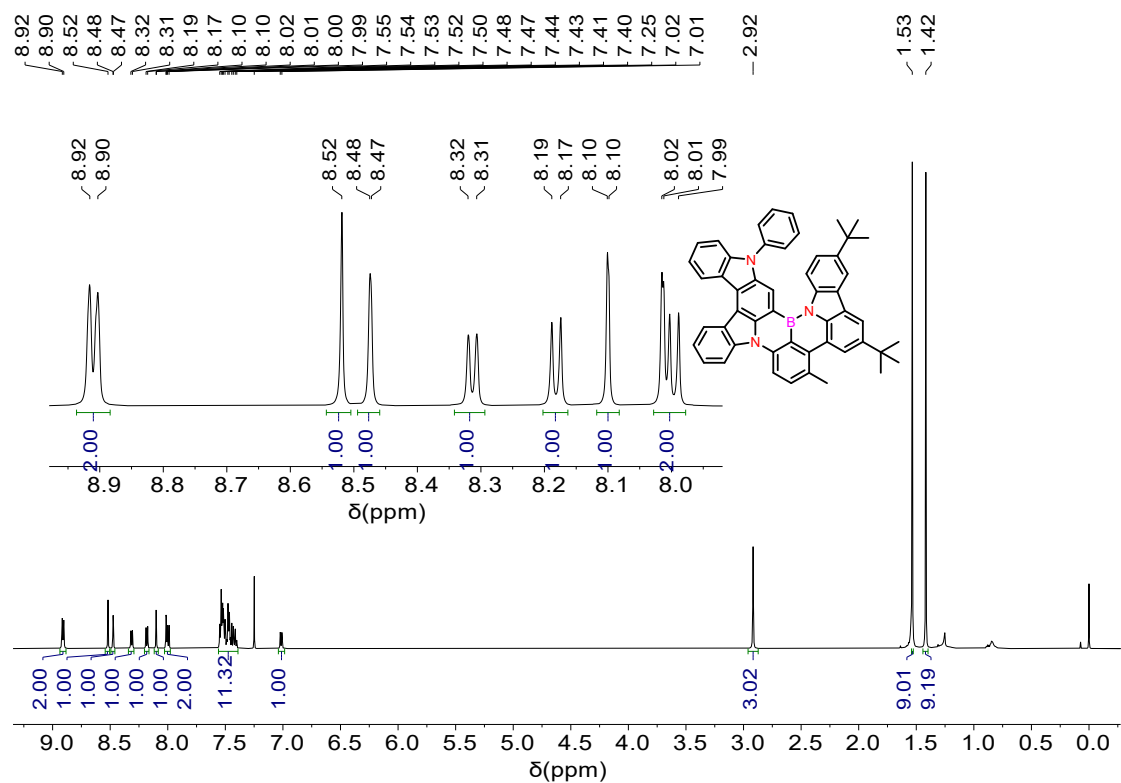


Figure S6. ^1H NMR spectrum of **ICz[B-N]** in CDCl_3 .

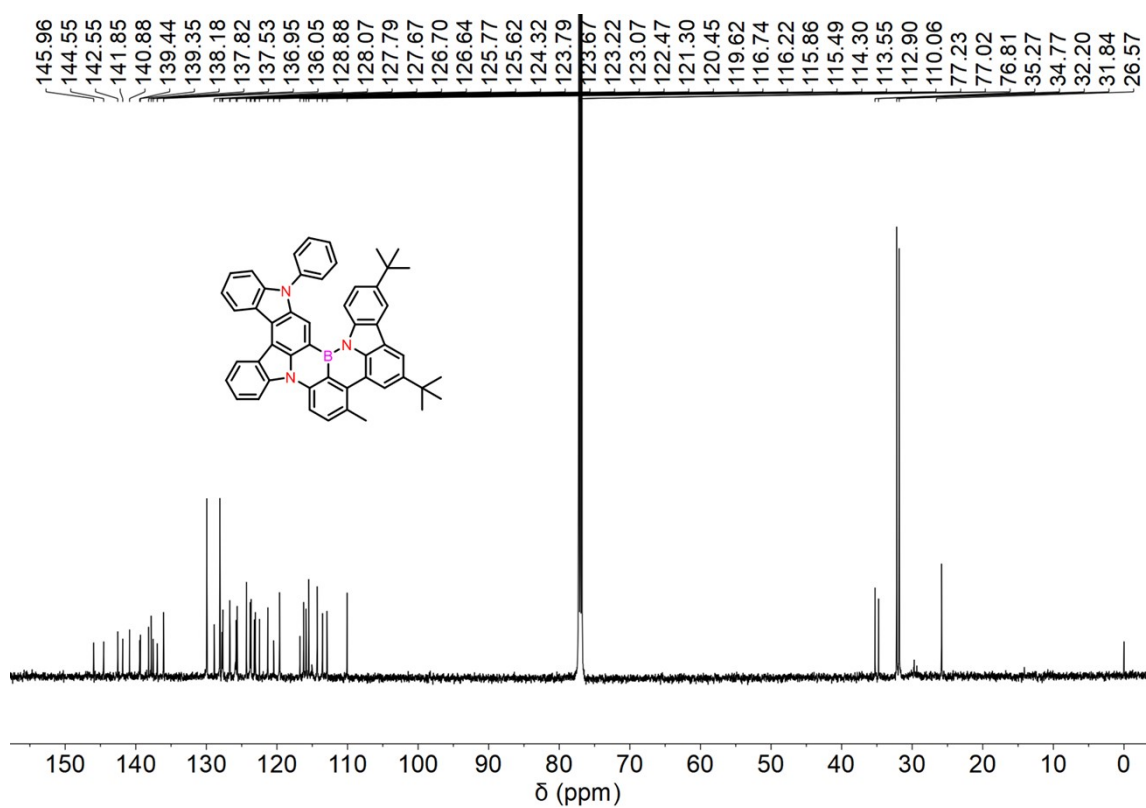


Figure S7. ^{13}C NMR spectrum of **ICz[B-N]** in CDCl_3 .

4. Reference

- [1] J.-D. Chai and M. H.-Gordon, *Phys. Chem. Chem. Phys.*, **2008**, 10, 6615.
- [2] L. Kronik, T. Stein, S. Refaely-Abramson, R. Baer, *J. Chem. Theory Comput.*, **2012**, 8, 1515.
- [3] H. Sun, C. Zhong, J. L. Brédas, *J. Chem. Theory. Comput.*, **2015**, 11, 3851.
- [4] Martin, R. L. Natural transition orbitals. *J. Chem. Phys.*, 2003, 118, 4775.
- [5] T. Lu, F. Chen, *J. Comput. Chem.* 2012, 33, 580.
- [6] W. Humphrey, A. Dalke, K. Schulten, *J. Mol. Graphics*, 1996, 14, 33-38.
- [7] a) Y. Wada, H. Nakagawa, S. Matsumoto, Y. Wakisaka, H. Kaji, *Nat. Photonics* **2020**, 14, 643; b) Q. Zhang, B. Li, S. Huang, H. Nomura, H. Tanaka, C. Adachi, *Nat. Photonics* **2014**, 8, 326.
- [8] G. Meng, H. Dai, T. Huang, J. Wei, J. Zhou, X. Li, X. Wang, X. Hong, C. Yin, X. Zeng, Y. Zhang, D. Yang, D. Ma, G. Li, D. Zhang, L. Duan, *Angew. Chem. Int. Ed.* 2022, 61, e202207293
- [9] G. Meng, H. Dai, J. Zhou, T. Huang, X. Zeng, Q. Wang, X. Wang, Y. Zhang, T. Fan, D. Z. Yang, D. Ma, D. Zhang, L. Duan, *Chem. Sci.* 2023, 14, 979–986.
- [10] G. Meng, J. Zhou, T. Huang, H. Dai, X. Li, X. Jia, L. Wang, D. Zhang, L. Duan, *Angew. Chem. Int. Ed.* 2023, 62, e202309923.
- [11] G. Meng, J. Zhou, X.-S. Han, W. Zhao, Y. Zhang, M. Li, C.-F. Chen, D. Zhang, L. Duan, *Adv. Mater.* 2024, 36, 2307420.
- [12] D. Wan, J. Zhou, Y. Yang, G. Meng, D. Zhang, L. Duan, J. Ding, Peripheral Substitution Engineering of MR-TADF Emitters Embedded With B–N Covalent Bond Towards Efficient BT.2020 Blue Electroluminescence. *Adv. Mater.* 2024, 36, 2409706.
- [13] X. Huang, J. Liu, Y. Xu, G. Chen, M. Huang, M. Yu, X. Lv, X. Yin, Y. Zou, J. Miao, X. Cao, C. Yang, *Natl. Sci. Rev.* 2024, 11, nwae115.
- [14] Y. Guo, W. Xie, Z. Ye, Ke Xu, Z. Zhang, Z. Xiao, J. Miao, Y. Zou, C. Zhong, X. Yin, C. Yang, X. Cao, *Angew. Chem. Int. Ed.* 2025, 64, e202503320.